PNAS
www.pnas.org

Supplementary Information for

TIP5 primes prostate luminal cells for the oncogenic transformation mediated by *PTEN*-loss

Karolina Pietrzak, Rostyslav Kuzyakiv, Ronald Simon[4], Marco Bolis, Dominik Bär, Rossana Aprigliano, Jean-Philippe Theurillat, Guido Sauter and Raffaella Santoro

Raffaella Santoro
Email: raffaella.santoro@dmmd.uzh.ch

This PDF file includes:

Supplementary text
Figures S1 to S6
Legends for Datasets S1 to S9
SI References

Other supplementary materials for this manuscript include the following:

Datasets S1 to S9

www.pnas.org/cgi/doi/10.1073/pnas.1911673117

Supplementary Information Text

Extended description of PCA analysis of organoids (Fig. 5A)

Principal component analysis (PCA) of RNAseq data from basal or luminal cells with different timing of *Pten* downregulation and *Tip5* deletion revealed similar differences observed by the phenotypic analysis reported above **(Fig. 5A)**. Along the first component (PC1 24.6%) of two-dimensional PCA analysis, both basal and luminal *Pten*-KD organoids were clearly separated from the corresponding control (shRNA-control) organoids, indicating that PCa organoids display distinct gene signatures. Interestingly, *Pten*-KD and control organoids of luminal origin were more separated compared to basal origin counterparts, suggesting that *Pten* downregulation has major effects in gene expression of luminal organoids than basal organoids. Remarkably, *Tip5*-KO→*Pten*-KD luminal organoids were closer to luminal control organoids than to *Pten*-KD organoids whereas *Tip5* KO→*Pten*-KD basal organoids were closer to *Pten*-KD basal organoids. These results are consistent with the data showing that *Tip5* depletion preceding *Pten* downregulation in luminal organoids impairs the *Pten*-mediated transformed phenotype whereas basal cells were less affected (**Fig. 4C-E**). Finally, gene expression profile of *Pten*-KD→*Tip5*-KO luminal organoids was closer to *Pten*-KD luminal organoids and distant from control and *Tip5*-KO→*Pten*-KD organoids, indicating that *Tip5* depletion after *Pten* downregulation has a minor effect once transformation is already initiated. Collectively, these results indicate that TIP5 plays a critical role for the initiation of PCa driven by *Pten*-loss, in particular in luminal cells, which are considered the cell of origin of aggressive PCa. In contrast, TIP5 is dispensable once the *Pten*-mediated transformation is established.

Methods.

Mouse strains and genotyping

Embryonic stem cells for the generation of *Tip5*-KO mouse lines were obtained from the EuMMCR (European Mouse Mutant Cell Repository). Blastocyst microinjection was conducted by Polygene AG (Rümlang, Switzerland). The *Tip5* knockout mice line (*Tip5*-KO) with constitutive deletion of *Tip5* alleles was generated by crossing *Tip5* $^{lox/lox}$ mice with *CMV-Cre* mouse line. Tamoxifen inducible model for conditional deletion of *Tip5* (*CMV-Cre-ER*^{T2}*; Tip5*$^{lox/lox}$) was generated by crossing *Tip5* $^{lox/lox}$ mice with *CMV-Cre-ER*^{T2} mice . Then, *CMV-Cre-ER*^{T2}*; Tip5*$^{lox/lox}$ mouse line was crossed with reporter ROSA26-mTmG$^{Tg/+}$ mouse line to obtain *CMV-Cre-ER*^{T2}*; Tip5*$^{lox/lox}$*;* ROSA26-mTmG$^{Tg/+}$ experimental animals. Upon treatment with 4-hydroxytamoxifen (4-OH Tam), Cre recombinase-mediated intramolecular rearrangement converts transgene expression of a cell membrane-localized red fluorescent protein (tdTomato/mT) into the expression of enhanced green fluorescent protein (GFP/mG). All mice used for crossing were obtained from The Jackson Laboratory and maintained on a C57BL/6N background. Genomic DNA was purified from toe tips (6 days old) by HotShot (1), and genotypes were determined by

PCR. All animal procedures were approved by veterinary authorities of Zurich and were performed in accordance with Swiss law.

Isolation of prostate epithelial cells

Isolation of prostate epithelial cells was performed as previously described (2). Murine prostate lobes were isolated from 10-11 weeks old mice under dissection microscope, macerated with blade and transferred into tube containing 1.5 ml solution of Collagenase/Hyaluronidase (Stem Cell Technologies) in ADMEM/F12 (Gibco Life Technologies) containing 100 µg/ml Primocin (InvivoGen). Subsequently, prostate tissue was incubated at 37°C rocking for 2 h. After collagenase digestion, samples were centrifuged at 350 g for 5 min, supernatant was discarded and cell pellet was washed with HBSS (Life Technologies). To dissociate prostate tissue into single cells, cell pellet was mixed with 5 ml TrypLE (Gibco Life Technologies) with the addition of 10 µM ROCK inhibitor Y-27632 (STEMCELL Technologies) and incubated for 15 min at 37°C followed by pipetting up and down several times. Subsequently, HBSS + 2% FBS (Gibco) (equal to 2x volume of TrypLE) was added to dissolve TrypLe and quench the reaction. Trypsinized prostate tissue was centrifuged at 350g for 5 min, supernatant was discarded, the pellet was washed with HBSS, and centrifuged again. 1 ml of pre-warmed Dispase/DNase I solution(STEMCELL Technologies) was added and samples were vigorously and continuously pipetted up and down until solution was homogenously translucent with no visible tissue fragments. Samples were centrifuged to remove Dispase solution and cell pellet was washed with ADMEM/F12 containing 2% FBS (equal to 5x volume of Dispase). To obtain single cells, suspension was filtered through a 40 um cell strainer, centrifuged and then supernatant was removed. Cells were resuspended in ADMEM/F12 + 2% FBS and viable cells were counted using hemacytometer and trypan blue.

FACS

Single cell suspension of prostate murine cells was obtained by filtration of trypsinized cells using 40-micron strainer as stated above. After incubation with 2% FBS in ADMEM/F12 for 10 min, cells were stained using CD49f-PE-Cy5 conjugated antibody (1:200, BD Pharmingen) and CD24-eFluor450 conjugated antibody (1:200, eBioscience) in 0.05% FBS in ADMEM/F12 supplemented with 10 µM ROCK inhibitor for 1h on ice in dark. Stained cells were centrifuged, and cell pellets were washed twice with HBSS, and re-suspended in ADMEM/F12 with 10 µM ROCK inhibitor. Basal and luminal cells were sorted on the basis of CD49f and CD24 expression, that was CD49f+/CD24-low for basal population and CD49f-low/CD24+ for luminal population. 1:300 dilution of 1 mg/ml Propidium Iodine (Sigma) was used to exclude dead cells for a downstream RNAseq analysis. Cells were sorted using BD FACSAria III (BD Biosciences).

Lentiviral transduction of organoids

Sequences encoding control shRNA (CACAAGCTGGAGTACAACTAC), shRNA targeting *Pten* (CGACTTAGACTTGACCTATAT) (2) were cloned into lentiviral vectors. Each lentivirus was generated using a one 10 cm plate of HEK293T cells. 10 ml of lentiviral supernatants were collected after 24 and 48 hours, centrifuged and frozen in -80°C over night. To enhance cell transduction, lentiviral supernatants were concentrated 100 times using Lenti-X Concentrator (Clontech) according to manufacturer's protocol. 40 µl of concentrated virus was mixed with 100.000 cells suspended in transduction medium (ADMEM/F12, B27 Glutamax, 10 mM HEPES, 100µg/ml Primocin, 2µg/ml Polybrene (Sigma-Aldrich), 10 µM ROCK inhibitor). Cells were incubated with virus for 20 min at RT, centrifuged for 40 min at 800 g at RT, and placed in incubator for 3.5 h to recover. Cells were plated in Matrigel at 5.000 cells/well density and after 3 days postseeding 1 µg/ml puromycin (Gibco) was applied to select organoids stably expressing shRNA-control or shRNA-*Pten*.

RNA purification, reverse transcription and quantitative PCR (RT-qPCR)

RNA was purified with TRIzol reagent (Life Technologies) according to the manufacturer's protocol. Reverse transcription was performed using RNA 500 ng and random hexamers and reverse-transcribed into cDNA using MultiScribe™ Reverse Transcriptase (Life Technologies). qRT-PCR was performed on a Rotor-Gene Q (Qiagen) using KAPA SYBR® FAST (Sigma). cDNA was diluted 1:5 and analyzed in triplicate by real time PCR with intron spanning primers pairs. Relative gene expression was determined by normalization to *Gapdh* or *Hprt*. Sequences for the primer used in qRT-PCR are listed in **Dataset S9**

RNAseq and data analysis

Total RNA for all downstream analyses was purified with TRIzol reagent (Life Technologies). The quality of the isolated RNA was determined with a Qubit® (1.0) Fluorometer (Life Technologies**,** California, USA) and a Fragment Analyzer (Agilent, Santa Clara, California, USA). Only those samples with a 260 nm/280 nm ratio between 1.8–2.1 and a 28S/18S ratio within 1.5–2 were further processed. The TruSeq Stranded mRNA (Illumina, Inc, California, USA) was used in the succeeding steps. Briefly, total RNA samples (100-1000 ng) were polyA enriched and then reverse-transcribed into double-stranded cDNA. The cDNA samples was fragmented, end-repaired and adenylated before ligation of TruSeq adapters containing unique dual indices (UDI) for multiplexing. Fragments containing TruSeq adapters on both ends were selectively enriched with PCR. The quality and quantity of the enriched libraries were validated using Qubit® (1.0) Fluorometer and the Fragment Analyzer (Agilent, Santa Clara, California, USA). The product is a smear with an average fragment size of approximately 260 bp. Libraries were normalized to 10nM in Tris-Cl 10 mM, pH8.5 with 0.1% Tween 20. The HiSeq 4000 (Illumina, Inc, California,

USA) was used for cluster generation and sequencing according to standard protocol. Sequencing were paired end at 2 X150 bp or single end 100 bp. The quality of the 120 bp single end reads generated by the machine was check by FastQC, a quality control tool for high throughput sequence data (3). The quality of the reads was increased by applying: a) SortMeRNA (4) (version 2.1) tool to filter ribosomal RNA; b) Trimmomatic (5) (version 0.36) software package to trim the sorted (a) reads. The sorted (a), trimmed (b) reads were mapped against the mouse genome (mm10) using the default parameters of the STAR (Spliced Transcripts Alignment to a Reference, version 2.4.0.1) (6). For each gene, exon coverage was calculated using a custom pipeline and then normalized in reads per kilobase per million (RPKM) (7), the method of quantifying gene expression from RNA sequencing data by normalizing for total read length and the number of sequencing reads. The clustering and principal component analyses (PCA) based on the RPKM values were performed using R (version 2.14.0). EdgeR (8) (version 3.12.0, common dispersion estimate) and DESeq2 (9) (version 1.10.0, dispersion estimate based on the "fit only" model) packages were used to assess the differential expression between the samples. Only genes with more than one read per million in at least three samples were conserved for the analysis**.** The functional annotation analysis of the differentially expressed genes was performed using DAVID (Database for Annotation, Visualization and Integrated Discovery) (10). Proportional Venn diagram were obtained using eulerr R package version 6.0.0, https://cran.r-project.org/package=eulerr (11) .

Larsson J (2019). *eulerr: Area-Proportional Euler and Venn Diagrams with Ellipses*. R package version 6.0.0, https://cran.r-project.org/package=eulerr.

Histology analysis

Tissues and organoids were fixed using 4% paraformaldehyde (PFA) overnight and then washed with 70% ethanol. Fixed organoids were pre-embedded in HistoGel (Thermo Fisher Scientific) to pellet organoids together. Tissues and organoid pellets embedded in HistoGel were processed with an automated tissue processor and subsequently embedded in paraffin wax according to standard techniques. Samples were sectioned at 4 µm onto SuperFrost® Plus (Thermo Scientific) microscope slides and air-dried 37 °C overnight for any subsequent immunohistochemistry or routine H&E staining.

Hematoxylin and Eosin staining

Hematoxylin and Eosin (H&E) staining was performed with PFPE (paraformaldehyde-fixed-paraffin-embedded) sections dewaxed in Xylene (Sigma-Aldrich), followed by rehydratation in descending percentages of ethanol for 1 min (100%, 95%, 90%, 70%, 50%) and subsequently washed with water. Sections were stained in hematoxilin for 3 minutes (MEDITE), washed 3

times with deionized water, followed by one wash step in Scott water, again washed with deionized water, and subsequently counterstained with eosin (MEDITE) for 1 minute. Sections were then dehydrated in ascending ethanol concentrations (50%, 70%, 90%, 95%, 100%), cleared with Xylene and mounted with mounting media.

Immunofluorescence analysis

Organoid sections were dewaxed in Xylene (3x 3 min), followed by rehydration steps in descending percentages of EtOH (3 min in 100%, 95%, 90%, 70%, 50%), and washed twice in PBS. Slides were boiled in sodium citrate pH 6.0 (10mM sodium citrate, 0.05% Tween 20) for 15 minutes and then allowed to cool to room temperature for 30 minutes. Slides were then washed in TBS and blocked for at least 1 hour in TBS + 2% BSA. Samples were next incubated with primary antibodies in blocking reagent at 4°C overnight and then washed 3 times with TBS. Fluorescently labeled secondary antibody was added to samples for 1 hour at RT. Slides were then washed with TBS, Hoechst stained (33258, Sigma-Aldrich), washed 3 more times in TBS and mounted with Fluoro-Gel (Electron Microscopy Sciences).

Following antibodies were used for staining on murine prostate tissue and organoids: K5 (1:100, Biolegend #905501), K8 (1:100, Biolegend #904801), p63 (1:50, Abcam #ab735). Immunofluorescent images were digitally recorded with a Leica DMI 6000 B microscope.

Immunohistochemistry

Immunohistochemistry was performed using BrightVision+ histostaining kit (Immunologic) according to manufacturer's protocol. Briefly, PFPE organoid sections were dewaxed, rehydrated, boiled in sodium citrate, washed in PBS, and blocked in blocking solution as described above. Samples were incubated with anti-Ki67 primary antibody (1:100, Abcam ab15580) overnight in blocking reagent at 4°C and then washed 3 times with PBS. Post-antibody Blocking solution was added for 15 min and samples were incubated at RT. Sections were washed twice with PBS and then were incubated for 30 min at RT with Poly-HRP-Goat anti Mouse/Rabbit IgG. After incubation sections were washed twice with PBS and were incubated with 3,3' Diaminobenzidine (DAB) mixture (Bright-DAB, Immunologic) for 8 min according to manufacturer protocol. After incubation organoid sections were rinsed in deionized water and mounted with Fluoro-Gel.

Western Blot

Samples were lysed using RIPA buffer (50 mM Tris-HCL pH 8.0, 150 mM NaCL, 0.1% SDS, 0.5% Na-Deoxycholate, 1% NP-40) containing complete protease (Roch) and phosphatase (PhosSTOP, Roche) inhibitors. Protein content was quantified using standard Bradford assay. 20 µg of protein was loaded on 12% polyacrylamide gels and subsequently transferred to a PVDF membrane. Membranes were probed with antibodies directed against pAKT (Ser473) (1:1000

Cell Signaling #4060), PTEN (1:1000 Cell Signaling #9559), GAPDH (1:2000 Santa Cruz #sc-25778), and TIP5 (1:1000 Diagenode #C15310090). Following washes membranes were incubated with secondary HRP conjugated antibodies (HRP horse anti-mouse 1:10,000 Vector Laboratories #PI-2000, and HRP goat anti-rabbit HRP 1:10,000 Vector Laboratories #PI-1000. Signal was visualized with ECL (G&E Healthcare).

Prostate cancer tissue microarray

The prostate cancer tissue microarray (TMA), methods and scoring criteria used to generate TIP5 immunohistochemistry and PTEN deletion data was previously described (12, 13). The TMA has been subsequently expanded to 17747 cancer samples (14). In brief, radical prostatectomy specimens were available from 17,747 patients, undergoing surgery between 1992 and 2015 at the Department of Urology and the Martini Clinics at the University Medical Center Hamburg-Eppendorf. All prostate specimens were analyzed according to a standard procedure, including a complete embedding of the entire prostate for histological analysis (15). Histopathological data were retrieved from the patients' records, including tumor stage, Gleason grade, nodal stage and stage of the resection margin. Follow-up data were available for a total of 14,667 patients with a median follow-up of 48 months (range: 1 to 275 months). Prostate specific antigen (PSA) values were measured following surgery and PSA recurrence was defined as a postoperative PSA of ≥0.2 ng/ml or increasing PSA values in subsequent measurements. The TMA manufacturing process was described earlier in detail (16, 17). In short, one 0.6mm core was taken from a representative tissue block from each patient. The tissues were distributed among 39 TMA blocks, each containing 129 to 522 tumor samples. For internal controls, each TMA block also contained various control tissues, including normal prostate tissue. Kaplan Meier curves were generated using biochemical (PSA) recurrence as the clinical endpoint. The log-rank test was applied to test the significance of differences between stratified survival functions.

Processing of RNA-Seq datasets and ssGSEA analysis

RNA-Seq data of primary PCa that were derived from Vancouver Prostate Centre (VPC) were reprocessed from raw files. Alignment to human reference genome (hg38) was per performed using STAR aligner (6) and quantified at gene-level using Gencode annotations (18). Raw counts were further processed in R statistical environment using DESeq2 pipeline (9). Normalized expression values for SU2C study (hybrid-capture RNA-seq) were retrieved from cBioportal. Single sample gene-set enrichment analysis (*ssGSEA*) was performed in R statistical environment using GSVA package (19).

Dataset used in this study

Primary PCa (n = 333), TCGA_PRAD (20). Primary PCa (n = 43), Vancouver Prostate Centre (VPC), ENA accession number PRJEB21092 (21). CRPC (n = 93), cBioPortal accession number prad_su2c_2019 (22).

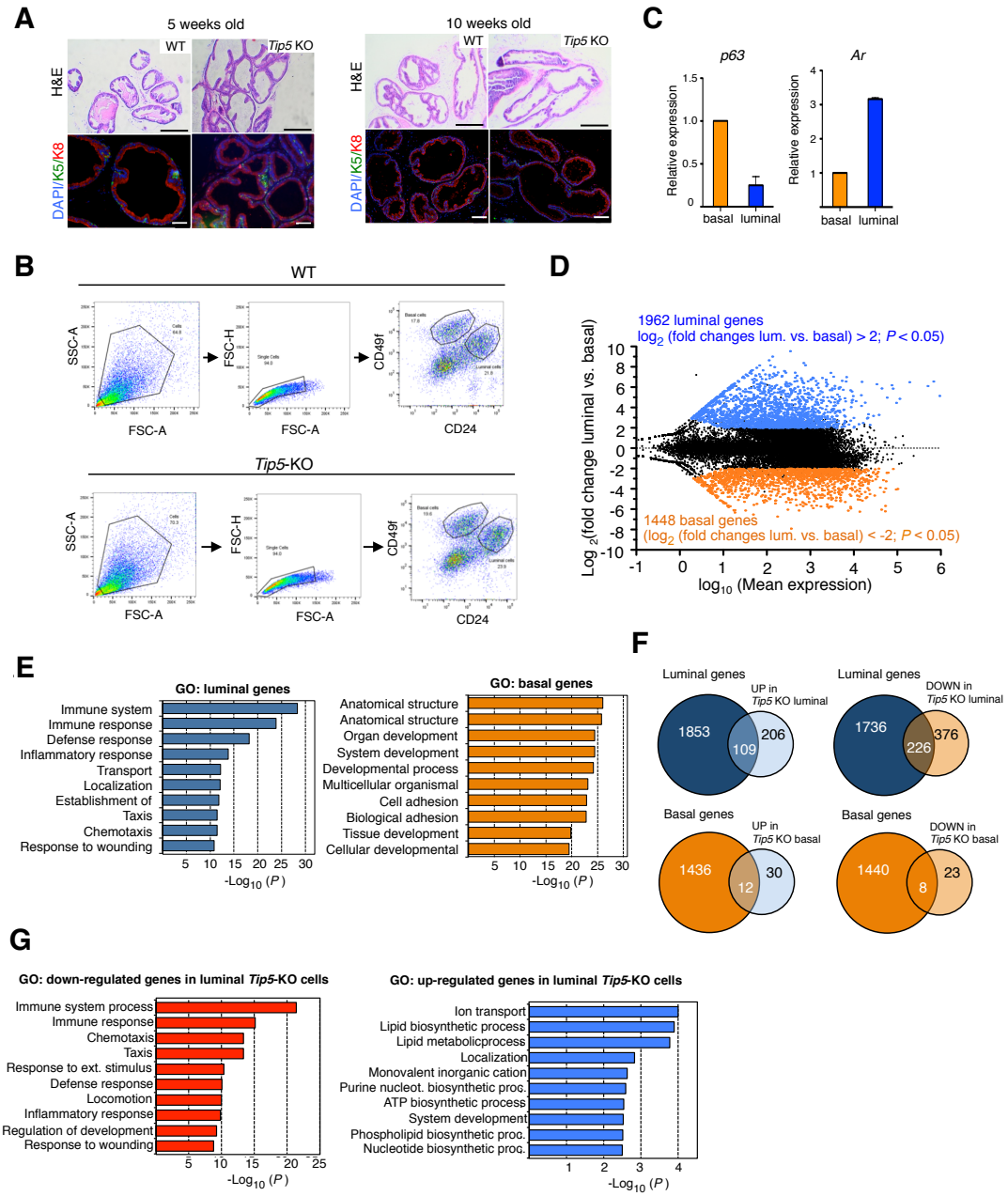

Fig. S1. TIP5 regulates luminal specific genes

A. Duct morphology and cell composition of 6 weeks and 10 weeks old WT and *Tip5*-KO mice is not altered in the absence of TIP5. H&E staining (top panel) and immunofluorescence with anti-K5 (green) and anti-K8 (red) (bottom panel) of mouse ventral prostate from 5 weeks old (left panel) and 10 weeks old (right panel) WT and *Tip5*-KO mice. Scale bars represent 200 µm (H&E) and 50 µm (IF). **B.** FACS gating strategy for the isolation of CD49f+/CD24-low (basal) and CD49f-low/CD24+ (luminal) stained WT and *Tip5* KO murine prostate cells. **C.** qRT-PCR expression analysis of *p63* and *Ar* in CD49f+/CD24-low (basal) and CD49f-low/CD24+ (luminal) cells. Expression was normalized to *Gapdh*. Average expression value of *p63* (3 experiments) and *Ar* (2 experiments). Error bars represent s.d. **D.** MA plots of RNAseq data showing differentially expressed genes between CD49f-low/CD24+ (luminal) and CD49f+/CD24-low (basal) WT cells. Luminal genes (blue dots) are defined on their significantly upregulation in luminal cells compared to basal cells (log_2-fold changes >2, *P* <0.05). Basal genes (orange dots) are defined on their

significantly downregulation in luminal cells compared to basal cells (log_2-fold changes < 2, P < 0.05). **E.** Top 10 significant GO terms of luminal and basal genes in WT prostate cells. **F.** Venn diagrams showing the number of differentially expressed genes upon *Tip5* deletion in basal or luminal cells compared to luminal or basal genes. **G.** Top 10 significant gene ontology (GO) terms as determined using DAVID for genes up- and down-regulated in *Tip5*-KO luminal cells.

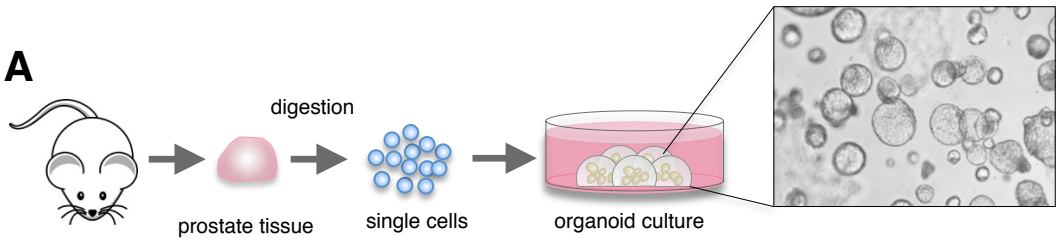
A
digestion
prostate tissue
single cells
organoid culture

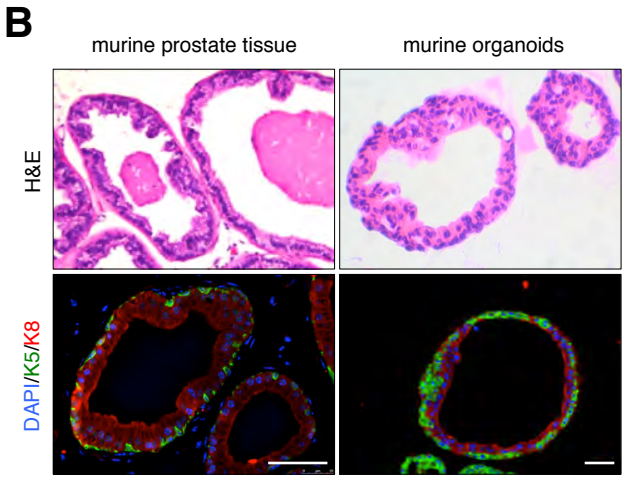
B
murine prostate tissue
murine organoids
H&E
DAPI/K5/K8

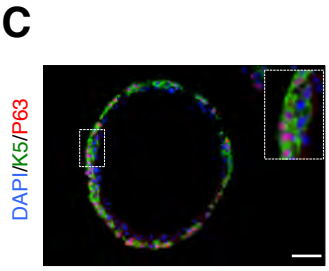
C
DAPI/K5/P63

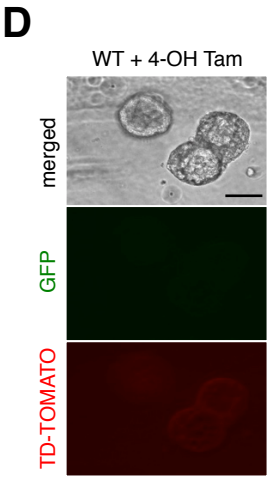
D
WT + 4-OH Tam
merged
GFP
TD-TOMATO

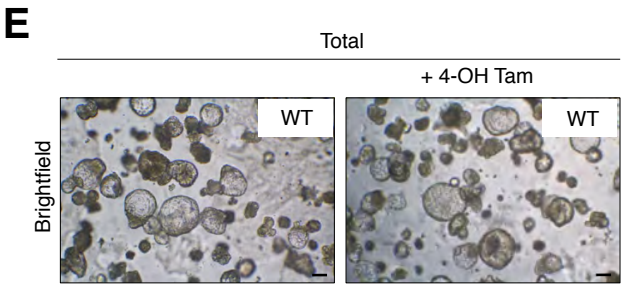
E
Total
+ 4-OH Tam
Brightfield
WT
WT

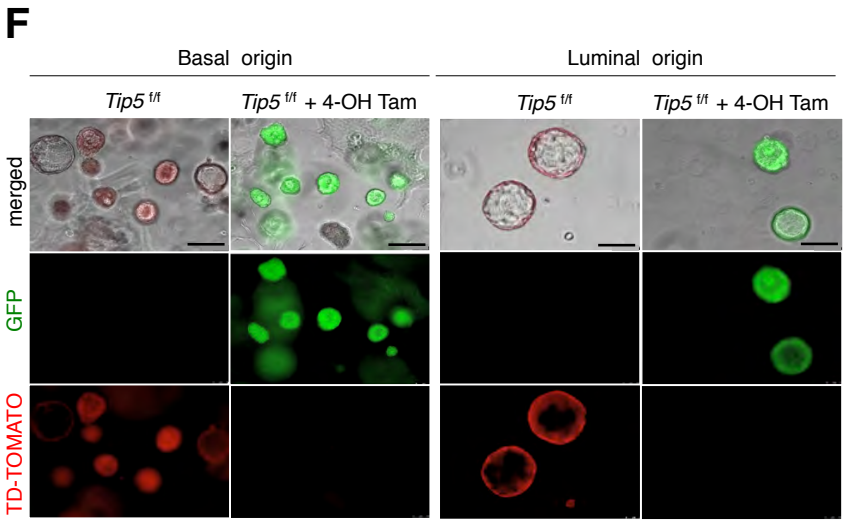
F
Basal origin
Luminal origin
Tip5 f/f
Tip5 f/f + 4-OH Tam
Tip5 f/f
Tip5 f/f + 4-OH Tam
merged
GFP
TD-TOMATO

Fig. S2. Mouse prostate organoids resemble the prostate gland

A. Scheme representing the generation of mouse prostate organoids. **B**. Mouse prostate organoids resemble the prostate gland. H&E staining (top panel) and immunofluorescence with anti-K5 (green) and anti-K8 (red) (bottom panel) of WT mouse prostate tissue (left panel) and mouse prostate organoids (right panel). Scale bars represent 200 μm (H&E) and 50 μm (IF). **C**. Immunofluorescence analysis with anti-K5 (green) and anti-p63 (red) of organoids derived from total (not-sorted) WT prostate cells. Scale bars represent 50 μm. **D.** Absence of GFP and dT-Tomanto fluorescence signal in organoids derived from WT mouse prostate cells and treated with 4-OH Tam. Scale bars represent 150 μm. **E.** Representative brightfield images of organoids derived from total (not-sorted) WT prostate cells treated with 4-OH Tam. Scale bars represent 150 μm. **F.** Fluorescent microscopy images showing the efficiency of TIP5 deletion in *Tip5* $^{f/f}$ luminal and basal cells as evident by the expression of GFP protein and loss of td-Tomato red protein signal upon 4-OH Tam treatment. Scale bars represent 150 μm.

.

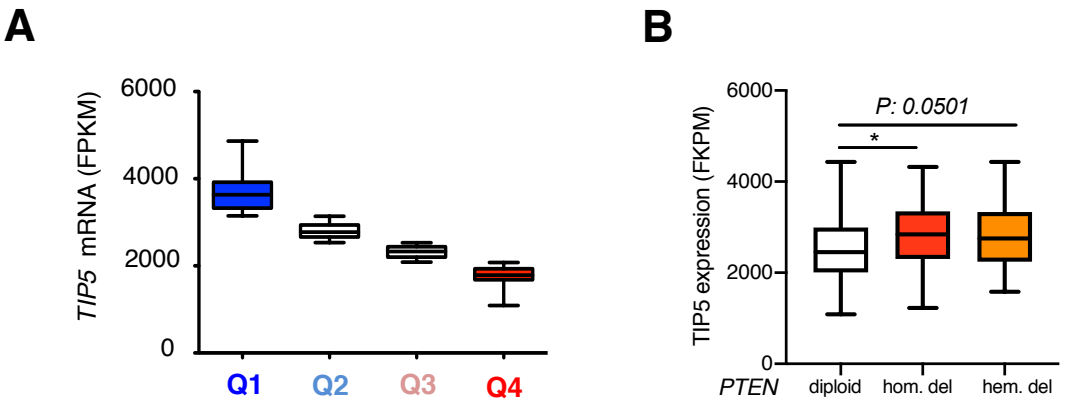

Fig. S3. TIP5 is highly expressed in primary tumors with *PTEN* deletion.
A. Annotation of patients into four groups based on *TIP5* expression in primary prostate tumors (n = 333), Q1 (n = 83), Q2 (n=84), Q3 (n = 83), Q4 (n = 83). Data are from the Cancer Genome Atlas Research (TCGA) Prostate Adenocarcinoma (PRAD) data (20). Expression is reported as fragments per kilo base per million mapped reads (FPKM value). **B.** *TIP5* expression in primary prostate tumors with *PTEN* homozygous (hom.) and hemizygous (hem.) deletions (del.). Data are from (20).

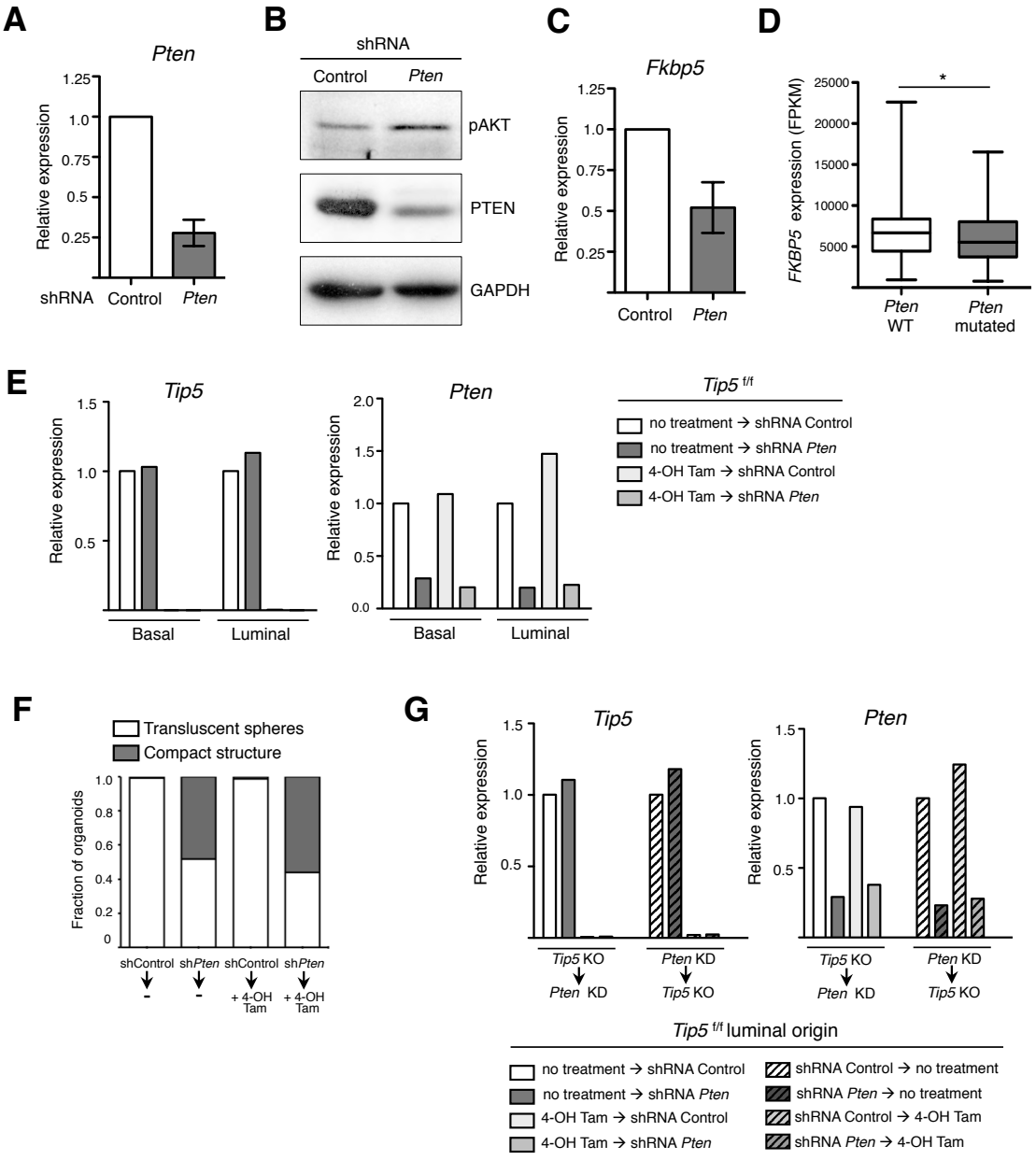

Fig. S4. Establishment of mouse basal and luminal organoids with *Pten*-downregulation
A. qRT-PCR expression analysis of *Pten* in shRNA-Control and shRNA-*Pten* transduced organoids. Values were normalized to *Gapdh* or *Hprt* mRNA levels. Average value of 3 experiments. Error bar represents s.d. **B.** Western blot analysis of PI3K activation in shRNA-Control and shRNA-*Pten* transduced organoids. GAPDH serves as loading control. **C.** qRT-PCR analysis of *Fkbp5* in shRNA-Control and shRNA-*Pten* transduced organoids. Values were normalized to *Gapdh* or *Hprt* mRNA levels. Average value of 3 experiments. Error bar represents s.d. **D.** *FKBP5* expression in primary prostate tumors with *PTEN* deletion. data are from the Cancer Genome Atlas Research (TCGA) Prostate Adenocarcinoma (PRAD). Expression is reported as fragments per kilo base per million mapped reads (FPKM value). **E.** qRT-PCR analysis of *Tip5* and *Pten* expression levels in organoids derived from basal and luminal *Tip5* $^{f/f}$ prostate cells treated with 4-OH Tam and followed by transduction with shRNA-Control or shRNA-*Pten* (*Tip5*-KO→*Pten*-KD organoids). Values were normalized to *Hprt* mRNA level. Data

are from one representative experiment. **F.** Quantification of morphology of *Pten*-KD and *Pten*-KD→*Tip5*-KO organoids of luminal origin. Results from n > 80 organoids per condition. Average of 3 independent experiments. **G.** qRT-PCR analysis of *Tip5* and *Pten* mRNA levels in a set of *Pten*-KD luminal organoids where *Tip5* deletion was performed prior (*Tip5*-KO→*Pten*-KD) or after (*Pten*-KD→*Tip5*-KO) to shRNA-*Pten* transduction. Values were normalized to *Hprt* mRNA level. Data from one representative experiment.

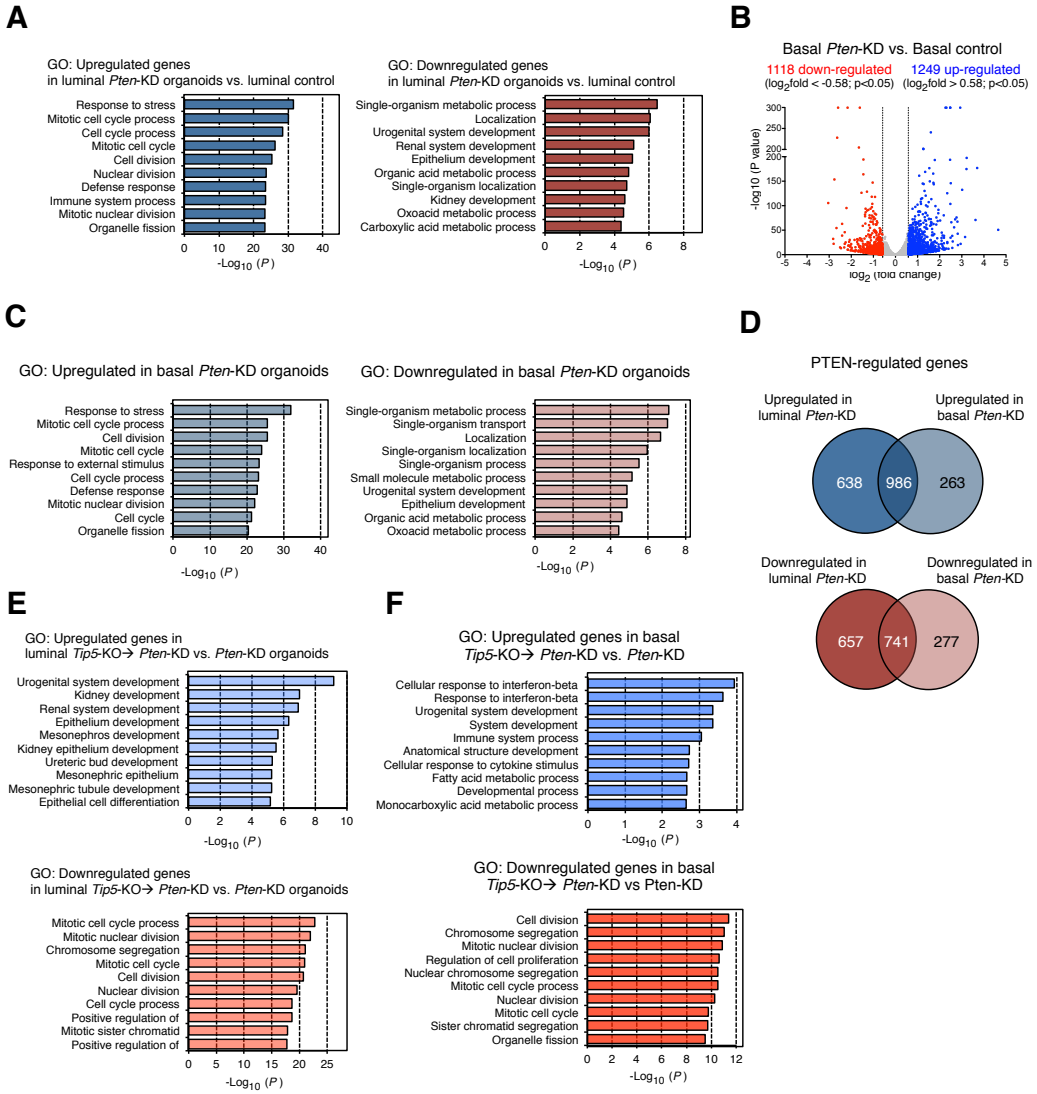

Fig. S5. A. Top 10 significant GO terms as determined using DAVID for differentially expressed genes upon *Pten* downregulation in luminal *Pten*-KD organoids versus luminal control organoids. **B**. Volcano plot showing the fold change (log_2 values) in transcript level of genes in basal *Pten*-KD organoids versus basal control organoids. Gene expression values of two replicates were averaged and selected for 1.5 fold changes and P<0.05. **C.** Top 10 significant GO terms for differentially expressed genes upon *Pten* downregulation in basal *Pten*-KD organoids versus basal control organoids. **D.** Venn diagrams showing the number of the commonly upregulated or downregulated genes between *Pten-KD* organoids of basal and luminal origin. **E.** Top 10 significant GO terms as determined using DAVID for differentially expressed genes in luminal *Tip5*-KO→*Pten*-KD organoids versus luminal *Pten*-KD organoids. **F**. Top 10 significant GO terms for differentially expressed genes upon *Tip5* deletion in basal *Tip5*-KO→*Pten*-KD versus basal *Pten*-KD organoids.

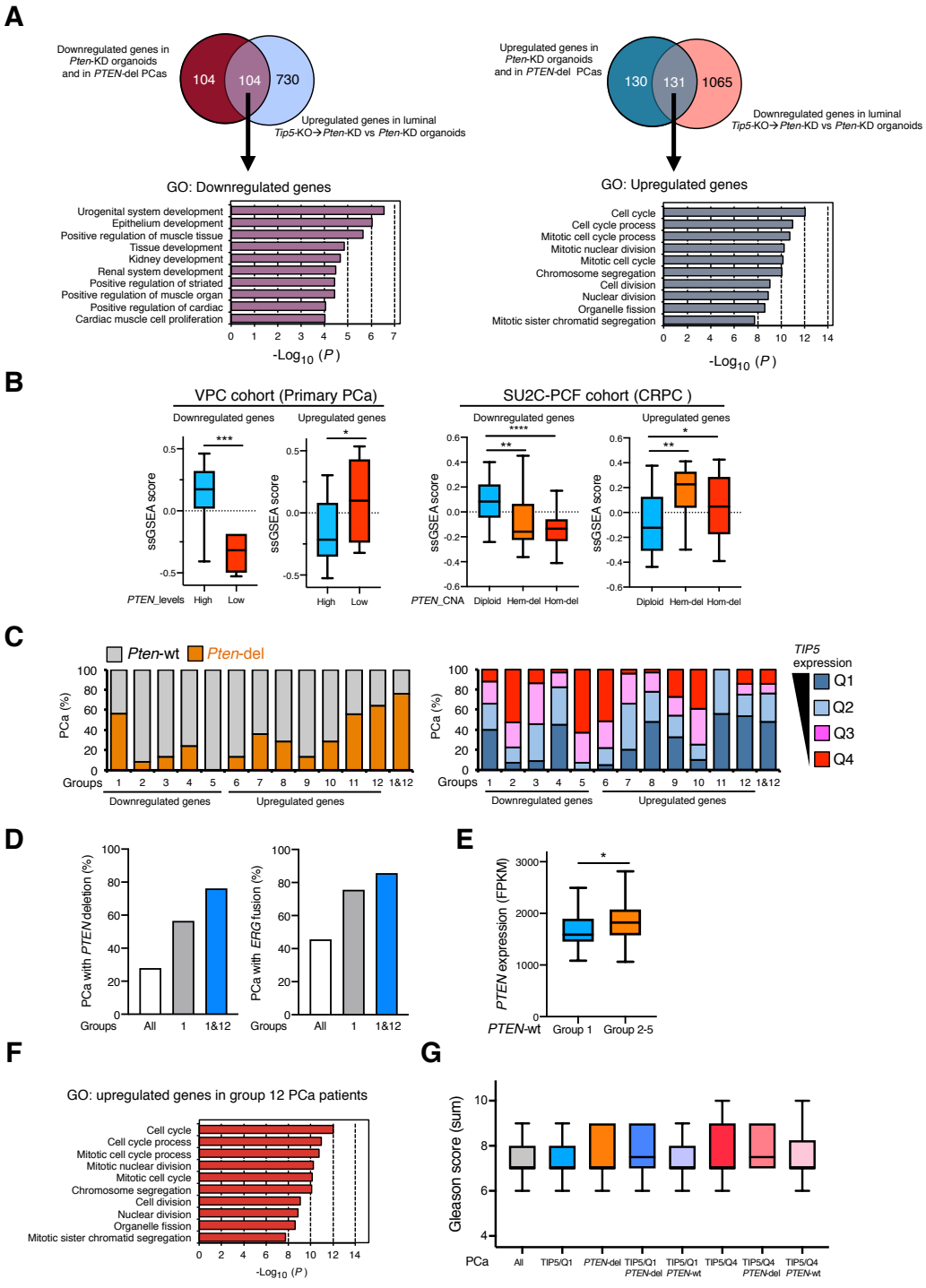

Fig. S6. A. Volcano plot showing the fold change (log_2 values) in transcript level of genes in basal *Pten*-KD organoids versus basal control organoids. Gene expression values of two replicates were averaged and selected for 1.5 fold changes and P<0.05. **B.** Top 10 significant GO terms for differentially expressed genes upon *Pten* downregulation in basal *Pten*-KD organoids versus basal control organoids. **C.** Venn diagrams showing the number of the commonly upregulated or downregulated genes between *Pten-KD* organoids of basal and luminal origin. **D**. Top 10

significant GO terms for differentially expressed genes upon *Tip5* deletion in basal *Tip5*-KO→*Pten*-KD versus basal *Pten*-KD organoids.

Dataset S1 (separate file).
RNAseq data for WT luminal and basal mouse prostate cells. List of genes upregulated (log_2-fold changes >2, *P* <0.05) and downregulated (log_2-fold changes <-2, *P* <0.05) in luminal cells compared to basal cells.

Dataset S2 (separate file).
GO terms for genes upregulated in WT luminal mouse prostate cells compared to basal cells and genes upregulated in WT basal mouse prostate cells compared to luminal cells.

Dataset S3 (separate file).
RNAseq data for *Tip5*-KO luminal and basal mouse prostate cells. List of genes upregulated (log_2-fold changes >0.58, *P* <0.05) and downregulated (log_2-fold changes <-0.58, *P* <0.05) in *Tip5*-KO basal cells compared to WT cells and *Tip5*-KO luminal cells compared to WT cells.

Dataset S4 (separate file).
GO terms for genes upregulated in *Tip5*-KO luminal mouse prostate cells compared to WT cells and genes upregulated in *Tip5*-KO basal mouse prostate cells compared to luminal cells.

Dataset S5 (separate file).
RNAseq data for organoids. List of genes upregulated (log_2-fold changes >0.58, *P* <0.05) and downregulated (log_2-fold changes <-0.58, *P* <0.05) in: luminal *Pten-KD* vs. luminal controlled organoids; basal *Pten*-KD vs. basal controlled organoids; luminal *Tip5*-KO→*Pten*-KD vs. *Pten*-KD organoids; basal *Tip5*-KO→*Pten*-KD vs. *Pten*-KD organoids; luminal *Pten*-KD→ *Tip5*-KO vs. *Pten*-KD organoids.

Dataset S6 (separate file).
GO terms for genes upregulated and downregulated in the following experimental organoid culture settings: luminal *Pten-KD* vs. luminal controlled organoids; basal *Pten*-KD vs. basal controlled organoids; luminal *Tip5*-KO→*Pten*-KD vs. *Pten*-KD organoids; basal *Tip5*-KO→*Pten*-KD vs. *Pten*-KD organoids.

Dataset S7(separate file).
List of genes related to Figure 5 and SI Appendix, fig. S5

Dataset S8 (separate file).
List of genes related to Figure 6 and SI Appendix, fig. S6.

Dataset S9 (separate file).
List of primers, antibodies, shRNA sequences and medium components used in this study.

References

1. Truett GE*, et al.* (2000) Preparation of PCR-quality mouse genomic DNA with hot sodium hydroxide and tris (HotSHOT). *Biotechniques* 29(1):52, 54.
2. Karthaus WR*, et al.* (2014) Identification of multipotent luminal progenitor cells in human prostate organoid cultures. *Cell* 159(1):163-175.
3. Andrews S (2010) FastQC: a quality control tool for high throughput sequence data.
4. Kopylova EN, L.; Touzet, H. (2012) SortMeRNA: Fast and accurate filtering of ribosomal RNAs in metatranscriptomic data. *Bioinformatics*.
5. Bolger A, M.; Lohse, M.; Usadel, B. (2014) Trimmomatic: A flexible trimmer for Illumina Sequence Data. *Bioinformatics*.
6. Dobin A*, et al.* (2013) STAR: ultrafast universal RNA-seq aligner. *Bioinformatics* 29(1):15-21.
7. Mortazavi A, Williams BA, McCue K, Schaeffer L, & Wold B (2008) Mapping and quantifying mammalian transcriptomes by RNA-Seq. *Nat Methods* 5(7):621-628.
8. Robinson MD, McCarthy DJ, & Smyth GK (2010) edgeR: a Bioconductor package for differential expression analysis of digital gene expression data. *Bioinformatics* 26(1):139-140.
9. Love MI, Huber W, & Anders S (2014) Moderated estimation of fold change and dispersion for RNA-seq data with DESeq2. *Genome Biol* 15(12):550.
10. Huang da W, Sherman BT, & Lempicki RA (2009) Bioinformatics enrichment tools: paths toward the comprehensive functional analysis of large gene lists. *Nucleic Acids Res* 37(1):1-13.
11. Larsson J (2019) eulerr: Area-Proportional Euler and Venn Diagrams with Ellipses. .
12. Gu L*, et al.* (2015) BAZ2A (TIP5) is involved in epigenetic alterations in prostate cancer and its overexpression predicts disease recurrence. *Nat Genet* 47(1):22-30.
13. Krohn A*, et al.* (2012) Genomic deletion of PTEN is associated with tumor progression and early PSA recurrence in ERG fusion-positive and fusion-negative prostate cancer. *Am J Pathol* 181(2):401-412.
14. Bonk S*, et al.* (2019) Prognostic and diagnostic role of PSA immunohistochemistry: A tissue microarray study on 21,000 normal and cancerous tissues. *Oncotarget* 10(52):5439-5453.
15. Schlomm T*, et al.* (2008) Clinical significance of p53 alterations in surgically treated prostate cancers. *Modern pathology : an official journal of the United States and Canadian Academy of Pathology, Inc* 21(11):1371-1378.
16. Kononen J*, et al.* (1998) Tissue microarrays for high-throughput molecular profiling of tumor specimens. *Nature medicine* 4(7):844-847.
17. Mirlacher M & Simon R (2010) Recipient block TMA technique. *Methods Mol Biol* 664:37-44.
18. Harrow J*, et al.* (2012) GENCODE: the reference human genome annotation for The ENCODE Project. *Genome Res* 22(9):1760-1774.
19. Hanzelmann S, Castelo R, & Guinney J (2013) GSVA: gene set variation analysis for microarray and RNA-seq data. *BMC Bioinformatics* 14:7.
20. Cancer Genome Atlas Research N (2015) The Molecular Taxonomy of Primary Prostate Cancer. *Cell* 163(4):1011-1025.
21. Ramnarine VR*, et al.* (2018) The long noncoding RNA landscape of neuroendocrine prostate cancer and its clinical implications. *Gigascience* 7(6).
22. Abida W*, et al.* (2019) Genomic correlates of clinical outcome in advanced prostate cancer. *Proc Natl Acad Sci U S A* 116(23):11428-11436.